(Received 24 October 2025, Accepted 8 December 2025, Scheduled 25 January 2026)

Methods for Evaluating PN Sequences in Spread Spectrum TDR

Phat Nguyen[1], Mouad Addad[1, 3, *], Samuel Makin[1], Joel Harley[2], Cynthia Furse[1], and Paul K. Kuhn[1]

[1] *Electrical and Computer Engineering Department, University of Utah, Salt Lake City, UT 84112, USA*
[2] *Electrical and Computer Engineering Department, University of Florida, Gainesville, FL 32611, USA*
[3] *Telecommunications and Digital Signal Processing Laboratory, Djillali Liabes University of Sidi Bel Abbes, SBA, Algeria*

ABSTRACT: This paper describes a Pseudo-Noise (PN) sequence evaluation tool that analyzes potentially corrupted PN sequences and assigns a metric score indicating the quality of the received sequence. The PN tester is designed to support Spread Spectrum Time Domain Reflectometry (SSTDR) by evaluating reflected PN sequences and determining whether the received signal is valid or too corrupted for use. Signal degradation is influenced by noise levels and channel filters encountered by the sequence. To simulate real-world conditions, various types of noise and filtering effects — representing capacitive or inductive coupling — were applied to a maximum-length PN sequence. The evaluation model demonstrated a consistent decline in correlation as signal distortion increased, confirming its effectiveness in assessing signal quality.

1. INTRODUCTION

Pseudo-random Noise (PN) sequences are used in Spread Spectrum Time Domain Reflectometry (SSTDR), which is a diagnostic method for detecting and monitoring faults in electrical wiring systems, such as those in aircraft, rail, instrumentation, power electronics, and photovoltaic panels [1, 2]. A modulated PN sequence is injected into a system under test (SUT), and the instrument monitors the signals reflected from the impedance discontinuities. It then cross-correlates the injected signal with the reflected signal to locate and characterize the faults.

As the signal passes through the system under test, it is degraded by various distortions such as attenuation [3], variability within the (SUT) [4–7] or electronics [8], noise [9], and capacitive or inductive (noncontact) coupling to the SUT [10–12]. These distortions can complicate signal analysis. Some of these distortions — such as reflections from faults — are precisely the changes SSTDR aims to detect. Others, including noise, attenuation, and coupling effects, are undesirable artifacts. Determining whether a received signal is reliable or excessively distorted can help quantify the confidence placed in its diagnostic value. The analysis can also be used as a metric to correct the received signal by applying corrective or adaptive filtering.

In both radar and communication systems, several standard methods are used to evaluate signal performance under noise and distortion. A *matched filter* is employed to optimally detect a known signal by maximizing the output *signal-to-noise ratio (SNR)* as established in detection and estimation theory and applied in radar and communication receivers [13–17]. In communication systems, the recovered signal quality is commonly quantified using metrics such as *bit error rate (BER)*, which characterizes the impact of noise and distortion on digital signal detection [16, 18]. For radar applications, the *ambiguity function* is used to characterize waveform properties and to assess resolution and distortion in time and frequency [13, 14, 17].

In this paper, we propose a method for evaluating the quality of the reflected PN code before using it for fault localization or other forms of data analysis. Since the original transmitted sequence is known, we assess the similarity between the transmitted and reflected sequences using the cross-correlation coefficient and key PN code properties — bit balance, run length, and bit correlation — and combine these into a composite quality metric that reflects the level of distortion. The remainder of this paper is organized as follows. Section 2 describes the PN sequence evaluation methods. Section 3 presents the testing procedures and results. Finally, Section 4 summarizes the findings and provides concluding remarks.

2. PN SEQUENCE EVALUATION METHODS

A PN sequence is a type of binary sequence widely used in spread spectrum communication, such as code division multiple access (CDMA) [19–21]. PN sequences are also employed in the SSTDR, where they are transmitted into an SUT, reflect off impedance discontinuities, and return to the tester. These reflected signals are cross-correlated with the original PN sequence to produce a correlation signature. Peaks in this signature correspond to reflections caused by impedance discontinuities, revealing their location, magnitude, and type [1, 2]. A key advantage of spread-spectrum signals is that PN codes can be distinguished from other signals and noise, enabling reliable operation in noisy or live (energized) environments. Additionally, multiple PN codes can be transmitted simultaneously, allowing concurrent communication or sensing channels and enabling multiple users to share the same bandwidth.

In this paper, we focus on Maximal Length (ML) sequences, which are a specific type of PN sequence, and evaluate the quality of received sequences based on distortions in their characteristic properties [22]:

* Corresponding author: Mouad Addad (addad.mouad@gmail.com).

1. *Bit Balance Property*: The number of ones in the sequence exceeds the number of zeros by exactly one. This measures the randomness of the sequence.
2. *Run Length Property*: A run is a sequence of identical digits (ones or zeros) occurring consecutively. An ML sequence contains runs that follow a predictable distribution in both length and frequency, determined by the code length.
3. *Bit Correlation Property*: If a complete ML sequence is cyclically shifted and compared bit by bit to the original sequence, the number of matching bits at each shift exceeds the number of mismatches by exactly one, and this property holds for every shift until a full cycle is completed. This measures the uniform predictability of the sequence.
4. *Cross-Correlation Property*: The cross-correlation coefficient quantifies the similarity between two sequences. This will be $+1$ for perfectly aligned identical sequences and -1 for inverted but perfectly aligned identical sequences.

Correlation-based criteria have traditionally dominated the evaluation of sequences in spread-spectrum systems. In CDMA systems [23, 24], sequences are selected and evaluated using periodic autocorrelation and cross-correlation functions to ensure reliable synchronization and to minimize multi-user interference [25–27]. In radar applications [13, 28], waveforms are assessed through their autocorrelation responses, with performance commonly summarized using sidelobe-based metrics such as peak sidelobe level and integrated sidelobe level. Similarly, SSTDR-related techniques evaluate PN sequences by analyzing the correlation peak between transmitted and reflected sequences, as this directly determines spatial resolution and noise robustness [29–32]. Various evaluation methods for these types of signals are summarized in Table 1.

TABLE 1. Summary of PN-sequence evaluation methods.

Appli.	Evaluation Method	Focus/Metrics
CDMA	Periodic autocorrelation & cross-correlation [23–27]	Synchronization, multi-user interference
Radar	Autocorrelation, sidelobe metrics [28, 30]	Range resolution, detection performance
SSTDR	Correlation peak between transmitted & reflected sequence [29–32]	Spatial resolution, noise robustness
This Work	Bit balance, Run Length, Bit-shift Correlation, Cross-Correlation	Sequence integrity after decoding

In this paper, we evaluate and score the four ML properties in the reflected sequence to assess the extent to which the ML code has been corrupted during transmission and reflection. These evaluations form the basis of a quality metric for the reflected ML code. Each metric can be applied independently or combined into a composite score that quantifies the integrity of the received sequence. The intent is to construct metrics that are sensitive to increasing distortions in the reflected PN codes.

2.1. Bit Balance Property

The Bit Balance property metric can be assessed by calculating the difference d between the number of ones and zeros in the reflected sequence. In an ideal ML sequence, this difference is exactly 1, reflecting the property that the number of ones exceeds the number of zeros by one. To evaluate how closely the reflected sequence preserves this property, we define a normalized metric as follows:

1. Take the absolute value of the observed difference, $|d|$, and subtract 1 to determine the deviation from the ideal.
2. Normalize this deviation by dividing by the maximum possible deviation, $N-1$, where N is the length of the sequence.
3. Subtract the normalized deviation from 1 to obtain a score that equals 1 when the bit balance is ideal and decreases toward 0 as the balance degrades.

This results in the following *Bit Balance Metric Score* (*BBMS*):

$$BBMS = 1 - \left(\frac{|d|-1}{N-1}\right) \tag{1}$$

This metric reaches a value of 1 when $|d| = 1$, indicating an ideal bit balance. An ambiguity with this formulation is that it assigns the same quality score to $d = 1$ (ideal case) and $d = -1$ (non-ideal case where zeros outnumber ones).

2.2. Run Length Property

Run Length refers to how many 0 s or 1 s occur in a row in an ML sequence. These patterns are well documented [19, 20]. To assess the Run Length property metric of an ML sequence, we compare the actual run length counts from the reflected sequence (the sequence under evaluation) to the run length counts (of both 1 s and 0 s) in the original sequence. For each valid run length, if the actual count from the reflected sequence matches the count from the original sequence, the *Run Match Factor (RMF)* is set to 1; otherwise, it is set to 0. The individual *RMFs* are then averaged to determine how closely the reflected sequence follows the ideal run length distribution. The Run Length Metric Score (*RLMS*) is:

$$RLMS = \frac{1}{(2n-2)} \sum_{i=1}^{n} (RMF_{1i} + RMF_{oi}) \tag{2}$$

where n is the order of the sequence; RMF_{1i} and RMF_{oi} are the *Run Match Factors* for run length i of 1 s and 0 s, respectively.

The *RLMS* ranges between [0, 1]. A value of 1 indicates a perfect match, where all run lengths in the reflected sequence exactly correspond to those in the original sequence. A value of 0 indicates no matches. Intermediate values represent partial matches, reflecting the degree to which the reflected sequence preserves the run-length distribution of the original sequence.

2.3. Bit Correlation Property

The Bit Correlation property metric can be assessed by shifting the reflected sequence cyclically bit by bit and comparing the resulting *shifted sequence* to the original non-shifted *reference sequence* for like bits in each bit position. For each shift: $i = 1$ to $N-1$, we track the number of *matching-bits* to *non-matching-bits*. We then assign a bit correlation shift score $BitC_i$ for each shift i as follows:

$$\begin{aligned} BitC_i &= 1 \quad \text{if } |\#\textit{matching-bits} - \#\textit{non-matching-bits}| = 1 \\ &= 0 \quad \text{otherwise.} \end{aligned}$$

The final *Bit Correlation Metric Score (BCMS)* is obtained by summing all the $BitC_i$ scores and dividing the total by $N-1$, thereby weighting each shift equally. This is expressed mathematically as:

$$BCMS = \frac{1}{N-1}\sum_{i=1}^{N-1} BitC_i \tag{3}$$

The resulting *BCMS* value lies in the range [0, 1]. A value of 1 indicates perfect adherence to the ideal bit correlation behavior expected of ML sequences, whereas a value of 0 indicates complete deviation. Intermediate values reflect a partial match.

2.4. Correlation Coefficient

A key metric for comparing the original and reflected ML sequences is correlation coefficient [22] which serves as the Cross-Correlation Coefficient Metric Score (CCMS). This coefficient quantifies the degree of similarity between the two sequences and is defined as:

$$CCMS = r_{xy} = \frac{\sum_{i=1}^{N}(x_i-\bar{x})(y_i-\bar{y})}{\sqrt{\sum_{i=1}^{N}(x_i-\bar{x})^2}\sqrt{\sum_{i=1}^{N}(y_i-\bar{y})^2}} \tag{4}$$

where N is the length of the sequence; x_i and y_i are the ith elements of the transmitted and reflected sequences, respectively; and $\bar{x}$ and $\bar{y}$ are the respective means of the transmitted and reflected sequences.

The Correlation Coefficient r_{xy} takes the values of -1 through $+1$. Values of -1 or $+1$ indicate a perfect correlation between the two sequences, whereas a value of 0 indicates no association. Negative values indicate the polarity of the association. Intermediate values reflect varying degrees of association. Unlike other quality scores used in this evaluation — such as Bit Balance, Run Length, and Bit Correlation — which are normalized to the range [0, 1], the *CCMS* spans a wider range of $[-1, 1]$. This broader scale captures both the strength and polarity of the linear association, which is useful for identifying inverse relationships in addition to direct matches. In the context of PN sequence evaluation, we can use the magnitude of the *CCMS* or $|CCMS|$, where $+1$ signifies the strong similarity between the transmitted and reflected sequences, and deviations from this ideal suggest potential distortion, noise, or corruption in the reflected signal.

2.5. Overall Quality Metric Score (QMS)

Each of the individual metric scores can be evaluated separately to assess specific types of degradation in the reflected ML sequence. These metrics target different structural properties of the sequence, and their individual evaluation can provide insights into where and how degradation has occurred. Alternatively, to obtain a unified measure of signal quality, these individual scores can be combined using a weighted sum. This results in an overall *Quality Metric Score (QMS)*, defined as:

$$\begin{aligned} QMS = W_{bb}BBMS + W_{rl}RLMS + W_{bc}BCMS \\ + W_{cc}|CCMS| \end{aligned} \tag{5}$$

where W_{bb}, W_{rl}, W_{bc}, and W_{cc} are the weighting factors assigned to the Bit Balance, Run Length, Bit Correlation, and Cross-Correlation respectively. These weights can be tuned to application-specific requirements or to sensitivity to specific types of sequence degradation.

In this paper, we focus on reflectometry for wire fault location. For this case, the correlation peak magnitude and its location are most important. For this, we will emphasize the correlation and de-emphasize the other metrics, by using the weights $W_{bb} = 0.0\%$, $W_{rl} = 22.5\%$, $W_{bc} = 22.5\%$, and $W_{cc} = 66.5\%$. The appropriateness of these weights was confirmed by preliminary results. The *CCMS* was weighted more due to its consistent baseline through the trials, while the *RLMS* and *BCMS* were equally weighted, but had observed variations, so we weighted them less than the CCMS. *BBMS* was set to 0, because the preliminary simulations showed minimal changes under the random noise and filtering trials, indicating an even 1s and 0s distribution under the inflicted distortions. This can be seen in the subsequent figures showing the metric changes versus distortions. The resulting *QMS* provides a normalized, composite measure of the reflected sequence quality. For other applications, such as those related to communication, where data is associated with individual bits, the other metrics may be weighted more. It may also be reasonable to consider only one of the metrics, in some cases, as opposed to combining them.

3. SIMULATION RESULTS

In real-world sensing systems, various types of degradation can compromise the integrity of ML sequence, leading to reduced accuracy in detection. To investigate the robustness of the proposed ML evaluation metrics, we simulated the system in Fig. 1 with several common forms of signal degradation. Additive White Gaussian Noise (AWGN) introduces random fluctuations in the reflected signal, which can corrupt individual bits, resulting in increased false correlations and degraded peak resolution [9]. Another source of degradation arises from elec-

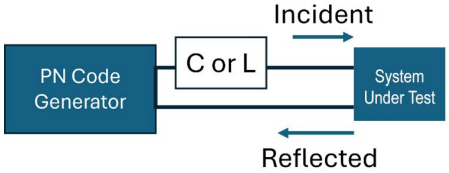

FIGURE 1. PN code generator with capacitive (C) or inductive (L) coupling to a transmission line or System Under Test (SUT).

tromagnetic coupling between the system components, such as when an instrument is indirectly coupled to a transmission line using capacitive, or inductive connection to the SUT [10–12]. Capacitive coupling introduces a high-pass filter effect, attenuating low-frequency components. Inductive coupling behaves as a low-pass filter, suppressing high-frequency components.

In this section, we will test the effectiveness of the evaluation method by simulating existing SSTDR instrumentation similar to that shown in Fig. 1. The SSTDR instrumentation generates a 2047-bit Manchester-encoded ML PN Code sequence transmitted into an SUT through capacitive and/or inductive coupling. The ML PN Code sequence originates as a 24 MHz and was generated using a linear feedback shift register (LFSR) with taps at positions 4, 5, 6, and 11. The sequence was then Manchester-encoded, yielding a 48 MHz signal. Degradation to the signal is applied in the SUT module by adding AWGN or by applying high-pass or low-pass filters digitally to simulate the capacitive or inductive coupling. The existing SSTDR instrument would typically correlate the received signal and analyze it from there. As we are interested in the reflected signal prior to the SSTDR instrumentation receiver port, in the lab, we capture the signal using an oscilloscope. The lab oscilloscope captures the signal with a 125 Mega-sample/second analog to digital converter probe at the output port of the SUT.

In our MATLAB simulations of the instrumentation described above, we generate the 48 MHz Manchester signal and sample it at 125 Mega-Samples/second (MS/s). The simulated AWGN is then added to this 125 MS/s signal. The capacitive and inductive couplings are typically analog mechanisms in the real world. The distortions due to these couplings are simulated by high-pass and low-pass filters applied at varying cutoff frequencies. To minimize artifacts in the signal processing step, we up-sampled the 125 MS/s signal to 1 GS/s. This signal was transformed into the frequency domain where the high-pass and low-pass filters were applied before transforming the filtered signal back to the time domain. This signal is then interpolated back to a 125 MS/s signal for decoding back to a PN Code via the Manchester decoder.

Once the 125 MS/s data is obtained, we decode the Manchester encoded signal by processing each 5-point windowed bit through a (Pearson) cross-correlation-based decoder. The samples are compared against two ideal five-sample Manchester '1' (a rising clock edge) and '0' (a falling edge) (IEEE encoding). We apply a 60% correlation threshold. If the correlation value between the sampled window and ideal Manchester templates exceeds this threshold, the corresponding bit value is recorded. However, if the sample is too noisy to meet the threshold for both comparisons, our simulation will flag the bit as an indeterminate value (NaN). Once the decoder has gone through the 125 MS/s signal and decoded as much as possible. It will then replace all indeterminate values with a random binary (0 or 1) to provide a complete 2047-bit sequence for metric evaluation.

3.1. Evaluation under White Gaussian Noise

In the presence of noise, the correlation properties of ML sequences will vary as a function of SNR. The ML sequences exhibit ideal autocorrelation in noise-free conditions [19], and that under AWGN, the correlation becomes statistical with a mean and variance that depend on SNR [16]. Metrics computed on the recovered binary sequence after Manchester decoding reflect these noise-induced deviations rather than the ideal correlation of the raw waveform [33]. As a result, the observed degradation of the Bit Correlation, Run Length, and Cross-Correlation metrics with decreasing SNR is consistent with the expected behavior of noisy ML sequences.

To assess the robustness of the proposed metrics, AWGN was added to the Manchester-encoded simulated analog signal and the Signal-to-Noise Ratio (SNR) was varied. Following noise injection, the sampled signal was decoded using a Manchester decoding algorithm to recover the digital bitstream. This recovered sequence was then compared to the original, noise-free ML sequence using the metric scores defined in Section 2. The effects of noise on each of these metrics, as a function of SNR, are presented in Fig. 2. The Bit Balance metric changed very little with respect to SNR, but the other three individual metrics responded well to this degradation. Of the responding metrics, the Bit Correlation metric decreased the most rapidly as noise increased. The Run Length and Cross-Correlation scores also decreased with increasing noise, but not as rapidly as the bit correlation score. The Overall score, based on the weights chosen, represented a reasonable summary of the three-responding metrics.

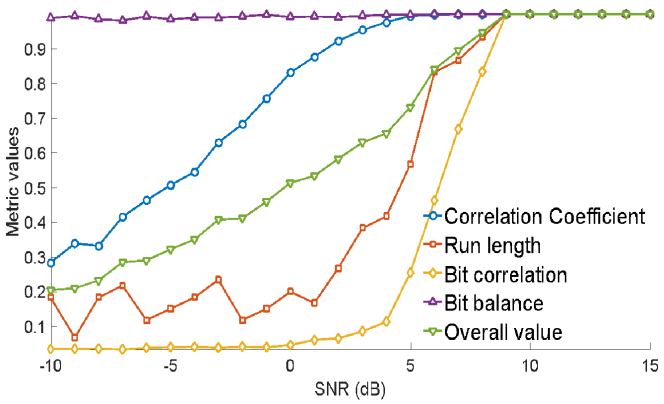

FIGURE 2. ML sequence evaluation under additive white Gaussian noise.

3.2. Evaluation under Inductive Coupling

To investigate the impact of low-pass filtering or inductive coupling, a low-pass filter was applied at varying cutoff frequencies in the simulation (method described above). The decoded sequence was compared to the unfiltered reference ML sequence to assess performance degradation across a range of filter cutoff frequencies. The resulting metric scores, which characterize the sensitivity of the system to inductive coupling variations, are summarized in Fig. 3. The Run Length, Bit Correlation, and Correlation Coefficient metrics showed considerable sensitivity and value reduction to the increasing cutoff frequency as the distortion increased. The Bit Balance again showed little change, and the Overall score showed an intermediate value with respect to the responding metrics.

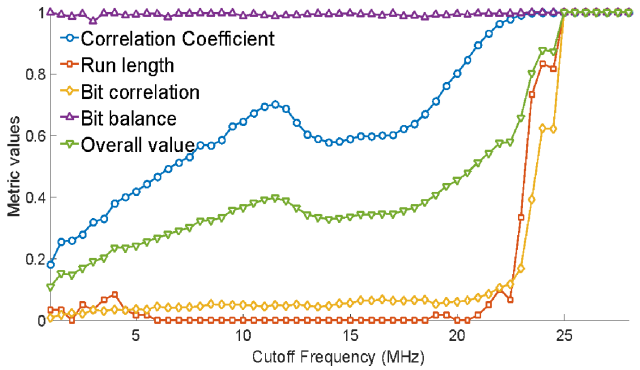

FIGURE 3. ML sequence evaluation distorted by low-pass filtering to represent inductive coupling.

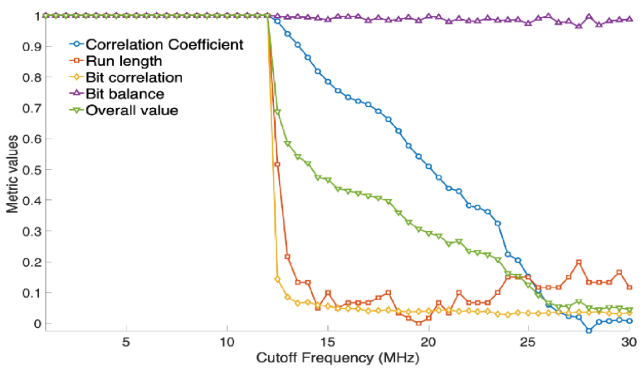

FIGURE 4. ML sequence evaluation distorted by high-pass filtering to represent capacitive coupling.

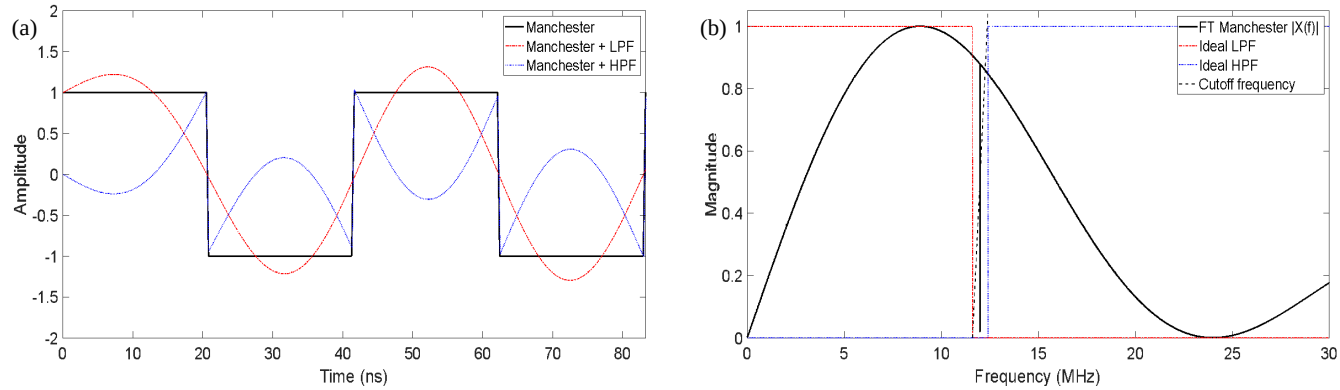

FIGURE 5. (a) Manchester-coded signal and filtering effects in the time domain. (b) Frequency-domain representation of a Manchester signal with ideal LPF and HPF.

3.3. Evaluation under Capacitive Coupling

To investigate the impact of high-pass filtering or capacitive coupling, a high-pass filter was applied at various cutoff frequencies in the simulation method described above. The decoded output was evaluated against the original ML sequence using the same metric scores, with degradation quantified across a range of cutoff frequencies. The results of the metric responses are shown in Fig. 4. The metrics under high-pass filtering showed sensitivity similar to that seen in the low-pass filter evaluation, with the Bit Balance metric showing little variations with the decreasing cutoff frequency .

The Manchester-coded signal is shown in the time domain together with the effect of filtering in Fig. 5(a)). A high-order FIR low-pass filter (LPF) is applied to illustrate how attenuation of high-frequency components (for instance, in the case of capacitive coupling) smooths the waveform and reduces the sharp transitions. A high-order FIR high-pass filter (HPF) is also shown to emphasize rapid transitions by suppressing low-frequency content (typical of inductive coupling, for instance). This diagram demonstrates the qualitative effect of bandwidth limitation on the Manchester waveform.

The frequency-domain representation is provided in Fig. 5(b). This shows the magnitude envelope of the Fourier transform of a 2047-bit 24 MHz ML PN sequence waveform. Manchester encoding doubles the frequency (to 48 MHz). This is overlaid with ideal low-pass and high-pass filter responses (with 12 MHz cutoff). The frequency-domain plot illustrates where the dominant spectral components of the Manchester signal lie and how filtering with different cutoff frequencies leads to the observed time-domain behavior. The asymmetry in the frequency-domain response shown in Fig. 5 leads to the asymmetry seen when comparing Figs. 3 and 4.

4. DISCUSSION & CONCLUSION

We constructed a PN code quality metric based on ML code properties, which shows sensitivity to distortions in the reflected code. We simulated AWGN, and capacitive and inductive coupling on encoded PN sequences and evaluated performance based on both individual and combined metric scores based on ML code properties. As the level of distortion increased, the corresponding metrics indicated degradation, confirming the tester's effectiveness in detecting loss in signal quality. For the distortions tested, the Bit Balance property was not a good measure, but the Run Length, Bit Correlation, and Cross-Correlation Coefficient metrics decreased as desired with increasing signal distortions. These results highlight the metrics' potential to identify signal degradation and provide a quantitative means of determining whether a reflected PN sequence remains viable for analysis. The metric has the potential to be used adaptively to process the signal to improve SNR and signal decoding.

CONFLICT OF INTEREST DISCLOSURE

Dr. C. M. Furse is a co-founder of LiveWire/Viper Innovation, which is commercializing SSTDR technology, and therefore she is disclosing a financial conflict of interest.

ACKNOWLEDGEMENT

We thank the Univ. of Utah Office of Undergraduate Research for supporting the research of P. Nguyen. M. Addad's work was supported by the U.S. Dept. of State through the Fulbright Visiting Scholar Program. The contents are solely the responsibility of the author and do not necessarily represent the official views of the Fulbright Program or the Govt. of the U.S.

REFERENCES

[1] Furse, C. M., M. Kafal, R. Razzaghi, and Y.-J. Shin, "Fault diagnosis for electrical systems and power networks: A review," *IEEE Sensors Journal*, Vol. 21, No. 2, 888–906, 2021.

[2] Kingston, S., E. Benoit, A. S. Edun, F. Elyasichamazkoti, D. E. Sweeney, J. B. Harley, P. K. Kuhn, and C. M. Furse, "A SSTDR methodology, implementations, and challenges," *Sensors*, Vol. 21, No. 16, 5268, 2021.

[3] Gazda, N., B. Paulsen, A. S. Edun, C. M. Furse, and J. B. Harley, "Reducing the effects of rain and moisture on spread spectrum time-domain reflectometry monitoring of photovoltaics," *IEEE Sensors Journal*, Vol. 24, No. 16, 26 181–26 189, 2024.

[4] Griffiths, L. A., R. Parakh, C. Furse, and B. Baker, "The invisible fray: A critical analysis of the use of reflectometry for fray location," *IEEE Sensors Journal*, Vol. 6, No. 3, 697–706, 2006.

[5] Makin, S., M. Addad, B. Redhead, and C. M. Furse, "Variability in spread spectrum time domain reflection and transmission measurements," *IEEE Transactions on Instrumentation and Measurement*, Vol. 74, 1–9, 2025.

[6] Harley, J. B., C. Liu, I. J. Oppenheim, and J. M. F. Moura, "Managing complexity, uncertainty, and variability in guided wave structural health monitoring," *SICE Journal of Control, Measurement, and System Integration*, Vol. 10, No. 5, 325–336, 2017.

[7] Kranold, L., M. Coates, and M. Popović, "Variability in clinical data obtained with flexible time-domain radiofrequency breast monitor," in *2018 18th International Symposium on Antenna Technology and Applied Electromagnetics (ANTEM)*, 1–3, Waterloo, ON, Canada, 2018.

[8] Morioka, T., "Systematic and random errors in the net power measurement using a reflectometer," *IEEE Transactions on Instrumentation and Measurement*, Vol. 70, 1–10, 2021.

[9] Benoit, E., J. Mismash, S. R. Kingston, A. S. Edun, H. Ellis, C. LaFlamme, M. A. Scarpulla, J. B. Harley, and C. M. Furse, "Quantifying the window of uncertainty for SSTDR measurements of a photovoltaic system," *IEEE Sensors Journal*, Vol. 21, No. 8, 9890–9899, 2021.

[10] Lee, Y. H., G.-Y. Kwon, and Y.-J. Shin, "Contactless monitoring technique for live shielded cable via stepped-frequency waveform reflectometry and inductive coupler," *IEEE Transactions on Industrial Electronics*, Vol. 69, No. 9, 9494–9503, Sep. 2022.

[11] Wu, S., C. Furse, and C. Lo, "Noncontact probes for wire faultlocation with reflectometry," *IEEE Sensors Journal*, Vol. 6, No. 6, 1716–1721, 2006.

[12] Zhao, Z. and K. Y. See, "A multiprobe inductive coupling method for online impedance measurement of electrical devices distributed in multibranch cables," *IEEE Transactions on Instrumentation and Measurement*, Vol. 69, No. 9, 5975–5977, Sep. 2020.

[13] Skolnik, M. I., *Radar Handbook*, 3rd ed., McGraw-Hill Education, 2008.

[14] Richards, M. A., *Fundamentals of Radar Signal Processing*, 2nd ed., McGraw-Hill Education, 2014.

[15] Van Trees, H. L., *Detection, Estimation, and Modulation Theory*, John Wiley & Sons, 2001.

[16] Proakis, J. G. and M. Salehi, *Digital Communications*, 5th ed., McGraw-Hill Education, 2007.

[17] Skolnik, M. I., *Introduction to Radar Systems*, 3rd ed., McGraw-Hill Education, 2001.

[18] Carlson, A. B. and P. B. Crilly, *Communication Systems*, 5th ed., McGraw-Hill Education, 2001.

[19] Golomb, S. W. and G. Gong, *Signal Design for Good Correlation: For Wireless Communication, Cryptography, and Radar*, Cambridge University Press, 2005.

[20] Brendle, Jr., J. F., "Pseudorandom code generation for communication and navigation system applications," [Online]. Available: https://apps.dtic.mil/sti/tr/pdf/ADA336311.pdf, 1997.

[21] Fan, P. and M. Darnell, *Sequence Design for Communications Applications*, Research Studies Press, 1996.

[22] Johnson, R. A., I. Miller, and J. E. Freund, *Probability and Statistics for Engineers*, Prentice-Hall, 2011.

[23] Sarwate, D. V. and M. B. Pursley, "Crosscorrelation properties of pseudorandom and related sequences," *Proceedings of the IEEE*, Vol. 68, No. 5, 593–619, May 1980.

[24] Simon, M. K., J. K. Omura, R. A. Scholtz, and B. K. Levitt, *Spread Spectrum Communications Handbook*, McGraw-Hill Education, 1994.

[25] Addad, M., A. Djebbari, and I. Dayoub, "Performance of ZCZ codes in QS-DS-CDMA communication systems," *Signal Processing*, Vol. 164, 146–150, Nov. 2019.

[26] Addad, M. and A. Djebbari, "Suitable spreading sequences for asynchronous MC-CDMA systems," *Journal of Telecommunications and Information Technology*, Vol. 3, 9–13, 2018.

[27] Addad, M. and A. Djebbari, "Adequate spreading codes to reduce MAI in quasi-synchronous MC-DS-CDMA system," *IET Communications*, Vol. 14, No. 12, 1992–1996, 2020.

[28] Levanon, N. and E. Mozeson, *Radar Signals*, 1st ed., John Wiley & Sons, 2004.

[29] Addad, M. and A. Djebbari, "Spread spectrum sensing based on ZCZ sequences for the diagnosis of noisy wired networks," *IEEE Sensors Journal*, Vol. 21, No. 2, 914–920, Jan. 2021.

[30] Addad, M. and A. Djebbari, "Simultaneous multiple cable fault locating using zero correlation zone codes," *IEEE Sensors Journal*, Vol. 21, No. 2, 907–913, Jan. 2021.

[31] Addad, M., A. Djebbari, E. Benoit, and C. M. Furse, "Analysis and experimental validation of SSTDR for simultaneous distributed diagnosis of wire networks," *IEEE Sensors Journal*, Vol. 25, No. 15, 29 630–29 637, Aug. 2025.

[32] Addad, M. and A. Djebbari, "Spread spectrum reflectometry for the simultaneous diagnosis of shielded cable bundles," *Nondestructive Testing and Evaluation*, Vol. 39, No. 4, 939–953, 2024.

[33] Sklar, B., *Digital Communications: Fundamentals and Applications*, 2nd ed., Prentice Hall, 2021.